Available online at www.sciencedirect.com
ScienceDirect
International Journal of Heat and Mass Transfer 51 (2008) 1104–1114
International Journal of HEAT and MASS TRANSFER
www.elsevier.com/locate/ijhmt

Effects of pressure gradients on entropy generation in the viscous layers of turbulent wall flows

Donald M. McEligot [a,b,c,*], Kevin P. Nolan [d], Edmond J. Walsh [d], Eckart Laurien [b]

[a] Aerospace and Mechanical Engineering Department, University of Arizona, Tucson, AZ 85721, USA
[b] Inst. für Kernenergetik und Energiesysteme (IKE), Uni. Stuttgart, Pfaffenwaldring 31, D-70569 Stuttgart, Germany
[c] Idaho National Laboratory, Idaho Falls, ID 83415-3885, USA
[d] Stokes Research Institute, Mechanical and Aeronautical Engineering Department, University of Limerick, Limerick, Ireland

Received 4 September 2006
Available online 15 August 2007

Abstract

By employing results of direct numerical simulations, it is possible to examine entropy generation due to friction in the viscous layers of turbulent flows with significant streamwise pressure gradients, both for boundary layers and channels. About two-thirds or more of the entropy generation per unit surface area S'' occurs there. Increasing the pressure gradient increases direct dissipation and decreases turbulent dissipation (in wall coordinates). The integral of the entropy generation rate per unit surface area to the edge of the viscous layer is relatively insensitive to pressure gradients for channels but decreases moderately for boundary layers.

Keywords: Entropy; Viscous layer; Turbulent; Channel; Boundary layer; CFD

1. Introduction

The local (pointwise) entropy generation rate per unit volume S''' is a key to improving many energy processes and applications [1]. In developing his reciprocal relations for irreversible processes, Onsager [2] extended Lord Rayleigh's "principle of least dissipation of energy" and indicated that the rate of increase of entropy plays the role of a potential. Thus, entropy generation (or "production" [3]) may be used as a parameter to measure a system's departure from reversibility. Bejan [1] has suggested that real systems which owe their thermodynamic imperfections to fluid flow, heat transfer and mass transfer irreversibilities be optimized by minimizing their entropy generation. This approach has been applied to compact heat exchangers, power plants, natural convection, rotating bodies, enhanced heat transfer surfaces, impinging jets, convection in general and other thermal systems.

Kock and Herwig [4] suggest that predicting the efficient use of energy in thermal systems requires accounting for the second law of thermodynamics since the loss of available work [5] is proportional to the amount of entropy produced (e.g., via the Gouy [6]–Stodola [7] theorem cited by Bejan). Therefore, apparatus producing less entropy by irreversibilities. destroys less available work, increasing the efficiency. Neumann et al. [8], Kock and Herwig and others are using computational fluid dynamics (CFD) codes to predict entropy generation for optimization by minimizing it. Since S''' determines the localized contribution to energy losses or reduction in the availability of energy [9,10], insight into the dominant loss sources and their locations can allow reducing them intelligently, thereby improving efficiency. These CFD studies seek to identify the regions of maximum entropy production so they may be attacked and reduced.

* Corresponding author. Address: Inst. für Kernenergetik und Energiesysteme (IKE), Uni. Stuttgart, Pfaffenwaldring 31, D-70569 Stuttgart, Germany. Tel.: +49 711 685 62495; fax: +49 711 685 62008.
E-mail address: Donald.McEligot@ike.uni-stuitgart.de (D.M. McEligot).

0017-9310/$ - see front matter © 2007 Published by Elsevier Ltd.
doi:10.1016/j.ijheatmasstransfer.2007.05.008

Nomenclature

A_{CS} flow area
D diameter
D_h hydraulic diameter, $4A_{CS}/P_W$
g_c units conversion factor, e.g., 1 kg m /(N s^2), 32.1739 lbm ft/(lbf s^2)
G mean mass flux, $\dot{m}/A_{CS}$
$\dot{m}$ mass flow rate
P perimeter; P_W, wetted perimeter
p pressure
$\dot{Q}$ heat transfer rate
s specific entropy (i.e., per unit mass)
S entropy, entropy generation rate
T temperature
U, V, W mean velocity components in streamwise, wall-normal and spanwise directions, respectively
V_b bulk or mixed-mean streamwise velocity, G/ρ
u, v, w velocity fluctuations about means in streamwise, wall-normal and spanwise directions, respectively
u_τ friction velocity, $(g_c\tau_w/\rho)^{1/2}$
$\overline{uv}$ Reynolds shear stress
x, y, z coordinates in streamwise, wall-normal and spanwise directions, respectively

Non-dimensional quantities
c_f skin friction coefficient, $2g_c\tau_w/(\rho U_\infty^2)$ or $2g_c\rho\tau_w/G^2$
K_p streamwise pressure gradient, $(\nu/\rho u_\tau^3)\mathrm{d}p/\mathrm{d}x$
K_v acceleration parameter, $(\nu/V_b^2)(\mathrm{d}V_b/\mathrm{d}x)$ or $(\nu/U_\infty^2)\mathrm{d}U_\infty^2/\mathrm{d}x$
Re Reynolds number, $4\dot{m}/\Pi D\mu$; Re_{Dh}, based on hydraulic diameter, GD_h/μ; Re_θ, based on momentum thickness, $U_\infty\theta/\nu$
Re_τ distance from wall to centerplane, centerline, etc., $y_c u_\tau/\nu$
$(S'')^+$ entropy generation rate per unit surface area, $TS''/(\rho u_\tau^3)$
$(S''')^+$ pointwise volumetric entropy generation rate, $T\nu S'''/(\rho u_\tau^4)$
y^+ distance from wall
ε^+ turbulent dissipation of turbulent kinetic energy, $\nu\varepsilon/u_\tau^4$

Greek symbols
δ boundary layer thickness
ε dissipation of turbulence kinetic energy; ε_u, pseudo dissipation [21]
Φ viscous dissipation function
μ absolute viscosity
ν kinematic viscosity, μ/ρ
ρ density
τ shear stress; τ_w, wall shear stress
θ momentum thickness

Superscripts
$(\_)^+$ normalization by wall units, ν and u_τ
$(\_)'$ per unit length
$(\_)''$ per unit surface area
$(\_)'''$ per unit volume
$(\bar{\ })$ time mean value

Subscripts
b bulk or mixed-mean quantity (one-dimensional)
c centerplane, centerline
cs cross section
cv control volume
Dh evaluated with hydraulic diameter D_h
gen generation
in evaluated at inlet, entry
out outflow
w wall
∞ freestream value

In the present study, we primarily examine entropy generation due to shear stresses in idealized "unheated," fully-developed, turbulent channel flows between infinitely-wide flat plates. However, for comparison purposes and to evaluate applicability of the results, we also treat two-dimensional turbulent boundary layers over a classical flat plate with both negligible and favorable pressure gradients in the streamwise direction. Fluid properties are idealized as constant.

We concentrate on the viscous layer because it is typically the region where the largest gradients occur and the production of turbulence is greatest. Following Bradshaw [11], we are here defining the viscous layer as the region where viscous effects are significant, but not necessarily dominant, typically to y^+ about thirty in a classical zero-pressure gradient case (it includes the "laminar" and "buffer" sublayers in some investigators's terminology). The major resistances to momentum, energy and mass transfer occur in this layer – and the pointwise entropy generation rate is greatest here as well.

As will be seen, turbulent channel flows with significant (non-dimensional) streamwise pressure gradients have low Reynolds numbers – and vice versa. Knowledge of such flows has been important in the design of the high temperature engineering test reactor (HTTR) in Japan since its flow rate is "low" to give a high outlet temperature Consequently, the outlet Reynolds number is about 3500 at design operating conditions. For other gas-cooled-reactors the low-Reynolds-number turbulent range can become important during natural circulation in decay heat removal by passive cooling and during hypothetical transient accident scenarios.

Kock and Herwig [4] applied the direct numerical simulations (DNS) of Kawamura et al. [12] for channel flow at $Re_\tau = 395$ to develop a relation for entropy generation in the viscous layer to be used with high-Reynolds-number CFD codes employing wall functions. With the DNS tabulations of Spalart [13,14], McEligot et al. [15] examined the effects of Reynolds number and favorable streamwise pressure gradients on entropy generation rates across turbulent boundary layers on flat plates. They found that, with negligible pressure gradients, results presented in wall coordinates are predicted to be *near* "universal" in the viscous layer while this apparent universality disappears when a significant pressure gradient is applied.

Key relations for evaluating entropy generation are presented in Section 2 which follows. They are applied first for the classical case of a negligible streamwise pressure gradient, found at high Reynolds numbers in channels, and then to favorable pressure gradients, approaching laminarization. The bases of the examination are the direct numerical simulations by Kawamura and coworkers [16,17] for fully-developed turbulent flow in channels and by Spalart [13,14] for external turbulent boundary layers. Comparison then allows determination when predictions of entropy generation from direct simulations of turbulent channel flows can and cannot be applied for the viscous layers of external turbulent boundary layers. We then summarize with some concluding remarks.

2. Background

Entropy appears in the second law of thermodynamics which can be written for a flowing open system, in terms of the "rate of creation" of entropy by London [18], as

$$\mathrm{RoC}(S) = S_{\mathrm{out}} + (\mathrm{d}S_{\mathrm{cv}}/\mathrm{d}t) - S_{\mathrm{in}} \geqslant \Sigma(\dot{Q}/T)$$

where $\dot{Q}$ is the rate of heat transfer into the control volume and T is the absolute temperature of the thermal reservoir from which this heat transfer comes. As a measure of the irreversibility, Bejan [1] and others define an entropy generation rate or rate of production of entropy [19]

$$S_{\mathrm{gen}} = \sum(\dot{m}s)_{\mathrm{out}} + (\mathrm{d}S_{\mathrm{cv}}/\mathrm{d}t) - \sum(\dot{m}s)_{\mathrm{in}} - \sum(\dot{Q}/T) \geqslant 0$$

which can be seen to be the inequality, if any, between $\mathrm{RoC}(S)$ and the reversible portion of entropy transfer with heat into the system. Possible irreversible processes are recognized to include friction, heat transfer with significant temperature gradients, combustion, etc.

For an isothermal, laminar pipe flow with no external heating imposed. Bejan [1] and others suggest that the volumetric entropy generation rate S''' can be estimated by evaluating the viscous dissipation function Φ for the flow,

$$S'''\{y\} = (\mu\Phi/T) = \mu(\partial U/\partial y)^2/T$$

Throughout the remainder of this paper, the streamwise velocity is represented as $U + u$, where upper and lower case letters symbolize its mean value and the instantaneous fluctuation about it, respectively; the normal velocity $V + v$ is treated in a similar fashion. (The braces { } are used to indicate that S''' is considered to be a function of y.)

The time mean value of $\mu\Phi$ at a point in a flow with turbulent fluctuations may be expanded to $\mu\Phi + \rho\varepsilon$ where the former represents viscous dissipation of mean-flow kinetic energy (called "direct dissipation") and the latter represents dissipation of turbulent kinetic energy into thermal energy ("indirect" or turbulent dissipation) [20–23].

$$\rho\varepsilon = 2\mu\left[\overline{\left(\frac{\partial u}{\partial x}\right)^2} + \overline{\left(\frac{\partial v}{\partial y}\right)^2} + \overline{\left(\frac{\partial w}{\partial z}\right)^2}\right] + \mu\left[\overline{\left(\frac{\partial u}{\partial x} + \frac{\partial v}{\partial x}\right)^2} + \overline{\left(\frac{\partial v}{\partial z} + \frac{\partial w}{\partial y}\right)^2} + \overline{\left(\frac{\partial w}{\partial x} + \frac{\partial u}{\partial z}\right)^2}\right]$$

When expressed in wall units, the pointwise entropy generation rate for a two-dimensional *boundary layer* can be written as

$$(S'''\{y^+\})^+ = [(\partial U^+/\partial y^+) + (\partial V^+/\partial x^+)]^2 + 2[(\partial U^+/\partial x^+)^2 + (\partial V^+/\partial y^+)^2] + \varepsilon^+$$

where $(S''')^+$ is defined as $T\nu S'''/(\rho u_\tau^4)$ and ε^+ is $\nu\varepsilon/u_\tau^4$. For a laminar boundary layer on a flat plate without freestream turbulence, S''' and its integrals can be calculated from the Blasius or Pohlhausen solutions [24]. For a *fully-developed* turbulent flow between infinitely-wide parallel plates this relation reduces to

$$(S'''\{y^+\})^+ = (\partial U^+/\partial y^+)^2 + \varepsilon^+$$

The mean velocity components V and W are identically zero for this idealization.

The prediction of pointwise entropy generation rate $(S'''\{y^+\})^+$ is desired to identify regions where most losses occur (large values of S''') and to deduce the entropy generation rate per unit surface area – and, ultimately, S' or S over the entire surface. In wall coordinates, the entropy generation per unit surface area value can be evaluated as

$$(S''\{y^+\})^+ = (TS''/(\rho u_\tau^3)) = \int_0^{y^+} (S'''\{y^+\})^+ \mathrm{d}y^+$$

Previous studies of turbulent flows with favorable streamwise pressure gradients have been summarized by Narasimha and Sreenivasan [25], Spalart [13], McEligot and Eckelmann [26] and others. Based on definitions, continuity and momentum equations and empirical relations, one can form approximate relations between some of the non-dimensional parameters suggested as governing flows with streamwise pressure gradients. Streamwise acceleration in a *boundary layer* is often represented by an acceleration parameter [27] defined as

$$K_{\mathrm{v}} = (\nu/U_\infty^2)\mathrm{d}U_\infty/\mathrm{d}x$$

For a boundary layer flow, one can show $K_v = -(c_f/2)^{3/2} K_p$ where K_p is the non-dimensional streamwise pressure gradient.

For *fully-developed turbulent flow in a duct*, K_v, is zero by definition and the pressure-gradient parameter may be estimated as

$$K_p = (v/\rho u_\tau^3)\mathrm{d}p/\mathrm{d}x \approx -20.1\ Re_{Dh}^{-(7/8)}$$

by employing a Blasius correlation [28]. Consequently, some authors may have interpreted "pressure-gradient effects" as "low-Reynolds-number effects" and others may not have realized that their fully-developed internal flow could have entailed significant streamwise pressure gradients. The distance y_c to the centerplane, centerline or other thickness measure can be represented as

$$y_c^+ = (y_c u_\tau/v) = (y_c/D_h) Re_{Dh} (c_f/2)^{1/2} \approx 0.20 (y_c/D_h) Re_{Dh}^{7/8}$$

This quantity is also denoted as Re_τ by some investigators (e.g., Kim et al. [29], Abe et al. [16]).

The likelihood of streamwise pressure gradients affecting the viscous layer was discussed by McEligot and Eckelmann [26]. The governing momentum equation for a two-dimensional boundary layer may be written as

$$U^+(\partial U^+/\partial x^+) + V^+(\partial U^+/\partial y^+) = -K_p + (\partial \tau^+/\partial y^+)$$

From this momentum equation, one sees the distribution of $\partial^+\tau\{y^+\}/\partial y^+$ will be a function of K_p alone provided the convective terms are zero or negligible. Fully-developed flows in tubes, parallel-plate channels and ducts inherently satisfy this requirement.

Near the wall, the solution for the total shear stress variation can be approximated [30,31] as

$$\tau^+\{y^+\} = (\tau\{y^+\}/\tau_W) = 1 + K_p y^+ [1 - (c_f/(2y^+)) \int_0^{y^+} (U^+)^2 \mathrm{d}y^+]$$

For a fully-developed flow in a duct or tube, the convective terms become zero as noted and this solution reduces to

$$\tau^+\{y^+\} = (\tau\{y^+\}/\tau_W) = 1 + K_p y^+$$

For a channel flow one can see that $-K_p = (1/y_C^+) = (1/Re_\tau)$. With $-K_p \approx 0$ ("large" Re_τ), the x-momentum equation reduces to $\tau^+\{y^+\} \approx 1$ near the wall, i.e., the constant shear layer assumption becomes valid, provided the flow thickness is "large" enough.

For the effect of a pressure gradient to be considered negligible in the viscous layer, one could establish a 5% criterion that τ^+ still be greater than 0.95 or such at its edge (say $y^+ \approx 30$). This constraint translates to requirements such as $-K_p < \sim 0.0017$, $Re_\tau > \sim 600$ and, for tubes or ducts, $Re_{Dh} > \sim 46{,}000$. McEligot and Eckelmann suggest that, for the viscous layer behavior to be similar in various geometries and flows, one needs (1) the viscous layer to be small relative to geometric scales in the flow and (2) to have the same distribution of $\partial\tau^+\{y^+\}/\partial y^+$ through the viscous layer. In a comparable study, Nieuwstadt and Bradshaw [32] showed that viscous layer statistics can be expected to be approximately equivalent in different geometries if their values of Re_τ are the same so that $\tau^+\{y^+\}$ would be about the same in both geometries (provided the outer boundary is not too close according to suggested criterion (1) above).

The works of Senecal [33], Patel [28], McEigot et al. [34], Spalart [13] and others have shown that the level of the mean velocity profile in wall coordinates increases with acceleration or a favorable pressure gradient. Fig. 1 demonstrates this effect for three channel flow cases [16,17] and two boundary layer flows [13] with varying pressure gradients when compared to the boundary layer calculation for $Re_\theta = 1410$ without acceleration and therefore with $-K_p$ identically zero [14]. The boundary layer predictions are indicated by long dashes with the result for zero pressure gradient (zpg) being the lowest. The channel flow predictions are shown by the solid curves and the trends are confirmed by the experiments of Thiele and Eckelmann [35] and Durst et al. [36]. Compared to the zero pressure gradient reference, all show an increase of $(U\{y^+\})^+$ in the viscous layer beginning near y^+ of ten and differing successively. For the boundary layer flows, one sees from the momentum equation that the convective terms counter the pressure gradient term so a given pressure gradient has less effect on the total shear stress $\tau^+\{y^+\}$ than the same pressure gradient for a channel flow. (This effect increases as y^+ increases so there is less difference for y^+ less than ten or so.) Consequently, the boundary layer profile at $-K_p \approx 0.0019$ differs less from the reference than does the channel case at $-K_p \approx 0.0013$ = a lower pressure gradient.

For fully-developed turbulent pipe flow at high Reynolds numbers, Bejan [1] derived an "universal" distribution of $(S'''\{y^+\})^+$ by assuming the three-layer von

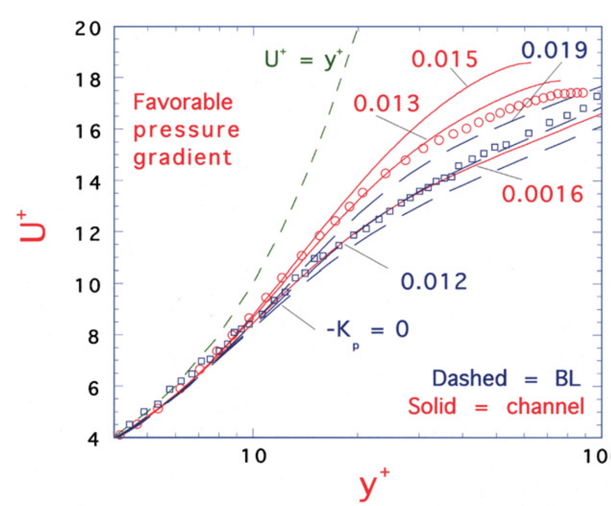

Fig. 1. Effects of favorable streamwise pressure gradients on mean velocity profiles in turbulent channel and boundary layer flows. DNS of Kawamura and coworkers for channels (solid curves) and Spalart for boundary layers (long dashes) compared to channel flow measurements at $-K_p \approx 0.006$ by Thiele and Eckelmann [35] and $-K_p \approx 0.0012$ by Durst et al. [36].

Karman "universal velocity profile." This assumption of an asymptotic high-Reynolds-number profile is equivalent to considering a low streamwise pressure gradient (lpg) and a constant shear layer $\tau\{y\}$ near the wall. He predicted that for $y^+ > 30$ the pointwise entropy generation rate would be less than 15% of its wall value, decreasing as y^+ increases (his Figure 3.6), and that the contribution of the turbulent dissipation would be about half the total (his Figure 3.8). As noted by McEligot and Eckelmann [26], for low values of $-K_p$ (e.g., "high" Reynolds numbers), the viscous layer of a turbulent boundary layer should show the same behavior as the viscous layer in a pipe or channel flow. Consequently, one would expect that for a turbulent boundary layer, entropy generation would again be concentrated in the viscous layer: the results of McEligot et al. [15] confirm this suggestion.

It is seen above that the viscous layer of a turbulent boundary layer is affected by both the streamwise pressure gradient and the convective terms. In the earlier paper, McEligot et al. showed that the entropy generation in the viscous layer is consequently affected. To evaluate the effects of pressure gradient *without the complication of streamwise acceleration, the primary objective* of the present study is taken to be the determination of the entropy generation in the viscous layers of fully-developed channel flows as the pressure gradient is varied. A range of about $0.0016 < |-K_p| < 0.016$ is provided by the simulations of Kawamura and colleagues.

3. Entropy generation with low pressure gradients

The reasoning above leads to the expectation that at "high" Reynolds numbers a channel flow will have the same behavior and, therefore, the same entropy generation in the viscous layer as an external boundary layer with negligible pressure gradient. The DNS of Spalart [14] at $Re_\theta = 1410$ provides a good representation of the latter case. The DNS database of Kawamura and colleagues for isothermal turbulent channel flow at $Re_\tau = y_c^+ = 640$ forms the basis of this comparison [16]; the flow was idealized as being fully-developed between infinitely-wide parallel plates with the Newtonian fluid having constant properties. This condition corresponds to $Re_{Dh} \approx 49{,}000$ and $-K_p \approx 0.0016$ for the streamwise pressure gradient. According to the order-of-magnitude reasoning of McEligot and Eckelmann [26], these viscous layer results should be reasonably applicable to any geometry provided the characteristic dimension is greater than about 600 in wall units, $-K_p < 0.0017$ and $Re_{Dh} > 46{,}000$. The reduction in total shear stress across the viscous layer is given by the quantity $30K_p$ or about 4.7% in this case, close to the constant shear layer approximation for an asymptotically-high Reynolds number. The calculations of Kock and Herwig [4] were for $Re_\tau = 180$ and 395 giving reductions of about 17% and 7.6% across the viscous layer, i.e., somewhat less constant.

The direct numerical simulation solves the governing Navier–Stokes and continuity equations in their three-dimensional, unsteady forms without modeling any terms. Consequently, it is not a "turbulence model." Kawamura and coworkers imposed periodic boundary conditions in the streamwise and spanwise directions with the no-slip condition at the walls. A finite difference method was adopted for solution with a fourth-order central difference scheme for the streamwise and spanwise directions and a second-order central difference scheme in the wall-normal direction. For time advancement, the Crank–Nicholson method was applied for viscous terms with wall-normal derivatives and the second-order Adams–Bashforth method was employed for other terms. The time integration for ensemble averaging corresponded to about 14 residence times after the flow reached a fully-developed state.

Spatial resolution for the grid was $\Delta x^+ = 800$, $\Delta z^+ = 400$ and Δy^+ was varied from 0.15 near the wall to about eight at the centerplane. The staggered computational grid of $1024 \times 256 \times 1024$ nodes covered a volume of $12.8y_c^+ \times 2y_c^+ \times 6.4y_c^+$.

From the Background considerations above, one sees that profiles of mean velocity and of the dissipation of turbulence kinetic energy are needed in order to calculate the pointwise entropy generation rate,

$$(S''')^+ = (\partial U^+/\partial y^+)^2 + \varepsilon^+$$

(The same relation evolves with boundary layer approximations.) Kawamura and others tabulate a "pseudo dissipation" ε_u^+ (in the terms of Gersten and Herwig [21]); citing Hinze [37], the desired dissipation ε^+ is called the "true dissipation" by Wilcox [38]. For a fully-developed channel flow, the difference is provided by a term common with viscous diffusion,

$$\varepsilon - \varepsilon_u = \nu(\partial^2\overline{v^2}/\partial y^2)$$

which, therefore, cancels in the governing equation for turbulence kinetic energy. From the DNS of Kim et al. [29] at $-K_p \approx 0.006$ ($Re_\tau \approx 180$), Bradshaw and Perot [39] show that the contribution of viscous diffusion is everywhere less than about 2% of the dissipation rate and conclude that the difference between the true dissipation rate and the pseudo dissipation rate can be ignored, for all purposes of computation and discussion.

In the present study we formed ε^+ by calculating the second derivative of $(\overline{v^2}\{y^+\})^+$ from Kawamura's (and Spalart's) listings and adding it to the tabulated ε_u^+. The term $(\overline{v^2}\{y^+\})^+$ is positive near the wall and becomes negative near y^+ about 15 and positive again at $y^+ > 160$. The resulting maximum difference between "true" and pseudo dissipation is about 2–1/2% at y^+ near five – where it is small relative to direct dissipation from the mean motion anyhow. A maximum negative value of about 1.3% occurs near the edge of the viscous layer.

The direct dissipation from the mean motion (labeled "Mean") and the turbulent dissipation ε^+ (labeled "Diss") are compared in Fig. 2. The logarithmic representation emphasizes the viscous layer while still giving indication of results well outside it. Logarithmic coordinates also

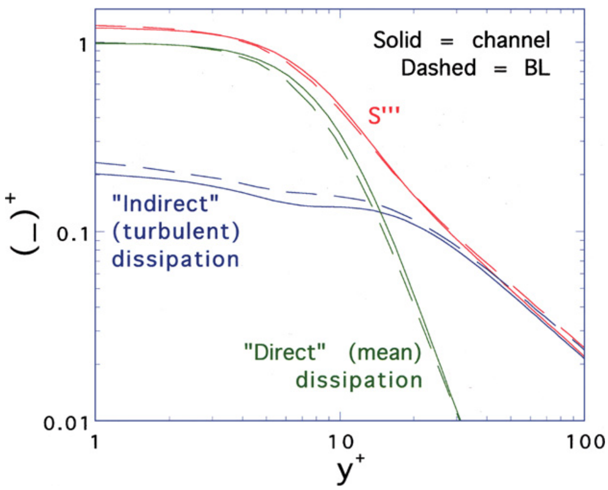

Fig. 2. Predictions of volumetric entropy generation rate and contributing terms for a channel flow with a low streamwise pressure gradient (solid curves) and a zpg boundary layer (dashed curves) from direct numerical simulations of Abe et al. [16] and Spalart [14], respectively.

make it easy to estimate per cent differences and, therefore, relative importance of terms. Solid curves represent the channel flow and the dashed ones are for the zpg boundary layer at $Re_\theta = 1410$. As expected, the channel predictions at high Re_τ agree closely, but not exactly, with those for the zpg boundary layer.

In wall coordinates the contribution of direct (mean) dissipation is unity at the wall. It dominates near the wall while turbulent dissipation contributes about 20% to the total. Consequently, the difference between true and pseudo dissipation corresponds to less than one-half per cent of the total in this region. Both direct and turbulent dissipation decrease as y^+ increases but the reduction of direct dissipation is more rapid with respect to y than the turbulent dissipation – so they become of about equal magnitude near $y^+ \approx 14$ or so. For larger values of y^+, turbulent dissipation becomes progressively more dominant. By the edge of the viscous layer the contribution of the mean motion is about negligible. Both direct and turbulent dissipation are seen to decrease rapidly beyond this region. Through the typical logarithmic layer and central core region the total dissipation and therefore the entropy generation are essentially provided by the turbulent dissipation.

In Fig. 1 the predicted mean velocity profile for the channel flow (solid, $-K_p \approx 0.0016$) is slightly higher than the reference boundary layer flow (dashed, $-K_p \approx 0$). Consequently, its direct (mean) dissipation is slightly greater for y^+ about three to the edge of the viscous layer. However, its indirect (turbulent) dissipation is less. These two countering results give close agreement for their sum $(S''')^+$ through the viscous layer: at $y^+ = 30$ the difference is only about 4%.

The pointwise entropy generation rate $(S''')^+$ is represented by the highest curve(s) in Fig. 2. Since it is the sum of direct and turbulent dissipation, in wall coordinates it is *of order* unity in the linear layer ($y^+ < \sim 5$) It then undergoes a sharp reduction through the rest of the viscous layer. By y^+ of thirty, the volumetric rate S''' is reduced to about eight percent of its value at the wall and it continues to decrease rapidly further away from the wall. This result agrees with the approximate prediction of Bejan [1] for a fully-developed, high-Reynolds-number pipe flow; his pipe flow would correspond to a low value of $-K_p$, the non-dimensional streamwise pressure gradient. Direct dissipation is reduced to less than one per cent of the wall value of total dissipation by $y^+ \approx 100$ but by then ε^+ is an order-of-magnitude greater than the direct dissipation so $(S''')^+ \approx \varepsilon^+$ there.

As noted in Section 2, the integral with respect to y of the pointwise entropy generation rate gives the entropy generation rate per unit surface area (S'') which would be sought by thermal fluid engineers. Fig. 3 demonstrates the increase of $(S''\{y^+\})^+$ through the viscous layer. Since $(S''')^+$ ranges only from about 1.2–0.9 in the linear layer ($y^+ < \sim 5$), the integral increases *nearly* linearly with respect to y in that region. About 30% of the entropy generation occurs in this layer. Beyond $y^+ \approx 5, S'''$ decreases sharply with respect to y. By $y^+ \approx 20$ the turbulent dissipation is significantly greater than the direct dissipation due to the mean motion so the contribution to S'' is then primarily from turbulent dissipation. For these conditions, the total $(S''\{y_c^+\})^+$ is about 19; by the edge of the viscous layer at $y^+ \approx 30$, approximately two-thirds has appeared (and about three-quarters by $y^+ \approx 50$). Beyond $y^+ \approx 100$ the distance to the centerplane is still large in well units, but $(S''')^+$ is small so the additional contribution to entropy generation per unit surface area $(S'')^+$ is likewise small.

The solid curve in Fig. 3 provides the prediction for the channel flow and again the dashed curve represents the reference boundary layer. While one can discriminate minor differences, consistent with, those in $(S''')^+$, they would

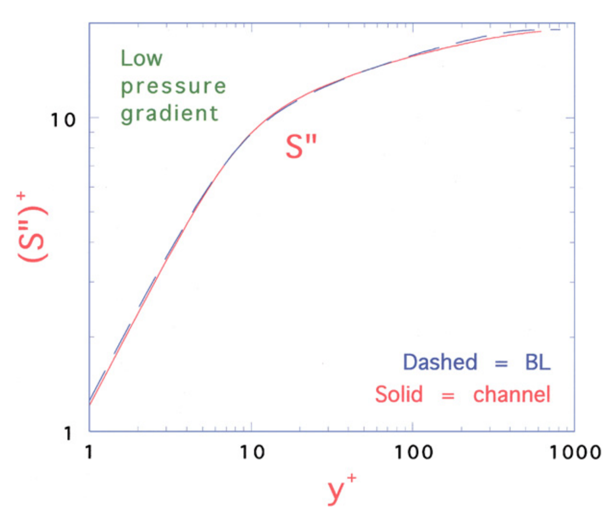

Fig. 3. Predictions of entropy generation rate per unit surface area for a channel flow with a low streamwise pressure gradient (solid curve) and a zpg boundary layer (dashed curve) from direct numerical simulations of Abe et al. [16] and Spalart [14], respectively.

not be considered significant At the edge of the viscous layer at $y^+ = 30$ the agreement is within one percent.

In summary, the viscous layer results of Abe et al. [16] at $Re_\tau = 640$ can be considered to be closely representative of the viscous layer of a high-Reynolds-number turbulent wall flow with negligible pressure gradient, particularly as S''' and S'' are concerned.

4. Entropy generation with favorable pressure gradients

As noted above, McEligot et al. [15] examined entropy generation in the viscous layers of turbulent boundary layers with favorable pressure gradients and found significant effects; in that case, the shear stress profile in the viscous layer is affected both by the streamwise pressure gradient and by convective terms in the x-momentum equation. Accordingly, to evaluate entropy generation in the viscous layer without the effects of the convective terms, the present study concentrates on fully-developed channel flows. Necessary quantities are provided for the range of about $0.0016 < |-K_p| < 0.016$ by the DNS databases of Kawamura and colleagues [16,17].

Fig. 1 and earlier studies demonstrate that the level of the mean velocity profile in wall coordinates increases with a favorable pressure gradient. Consequently, the contribution of direct dissipation from the mean motion can be expected to be greater with a favorable pressure gradient than without. While the effect of the term $-K_p y^+$ decreases the direct dissipation in the linear layer (via $\partial U^+/\partial y^+$), one sees from the slope of the mean velocity profile at larger y^+ that this effect is more than compensated by reduction of turbulent momentum transfer as the pressure gradient increases.

For a two-dimensional boundary layer the terms for production in the governing equation for turbulence kinetic energy are

$$-\rho[\overline{u^2}(\partial U/\partial x) - \overline{v^2}(\partial U/\partial x) + \overline{uv}\{(\partial U/\partial y) + (\partial V/\partial x)\}]$$

As indicated by Hinze [37], for a flow with velocity increasing in the x-direction the first term promotes a decrease in turbulence kinetic energy. With less production, there is less turbulence kinetic energy to dissipate and the turbulent dissipation term can be expected to decrease as well.

For the terms in the balances of Reynolds stresses near the wall, Spalart [13] noted that the general levels were lower in sink flow as implied. So the turbulent dissipation should be reduced. The results of McEligot et al. confirmed this expectation for turbulent boundary layers with favorable pressure gradients.

Antonia et al. [40] examined turbulent dissipation and models thereof for turbulent channel flows at $Re_\tau = 180$ and 395 ($-K_p \approx 0.0056$ and 0.0025, respectively) as predicted by the DNS algorithm of Kim et al. [29]. Their results show that, for this limited range, ε^+ decreased as $|-K_p|$ increased, consistent with the observations of Spalart [13] for boundary layers.

The present comparisons are based on application of the DNS databases of Kawamura and coworkers. Abe et al. [16] treated $Re_\tau = 180$, 395 and 640 ($0.0056 < |-K_p| < 0.0016$) as described earlier and their tabulations are currently available on an Internet web site maintained by Kawamura. Tsukahara et al. [17] extended these results to $-K_p \approx 0.016$ ($Re_\tau = 64$); at their highest pressure gradients these flows show some characteristics which could be considered to be "transitional." At $Re_\tau = 80.70$ and 64 the predicted skin friction coefficients diverge below accepted turbulent correlations and there are slight, reductions in the profiles of the streamwise turbulence intensities. At $Re_\tau = 80$, time series traces of u- and v-fluctuations show evidence of "turbulent puffs" [41]. For $Re_\tau = 110$ and above ($-K_p \approx 0.009$ and $Re_{Dh} \approx 6600$) good agreement was found with the correlation of Dean [42]. These results are in agreement with the measurements of Durst et al. [36] who found close agreement with the correlation of Dean for $Re_{Dh} = 6000$ ($Re_\tau = 102$) and above – and found comparable behavior of the streamwise turbulence intensities.

The effects of favorable pressure gradients on the two contributions to entropy generation are demonstrated in Fig. 4 for a range of cases. As implied by the mean velocity profile behavior, direct dissipation (labeled "Mean") from the mean motion increases with respect to pressure gradient in the viscous layer. Near $y^+ \approx 20$, it is about 40% greater for $-K_p \approx 0.009$ ($Re_\tau = 110$) and over 200% greater for $-K_p \approx 0.016$ ($Re_\tau = 64$) than for the lpg reference at $Re_\tau = 640$. However, the contribution from turbulent dissipation (labeled "Diss") decreases as $|-K_p|$ increases. Presumably, if $|-K_p|$ were large enough – say greater than 0.025 or so [26], the flow would laminarize so turbulence and its dissipation would disappear. While there is little effect on direct dissipation from increase of $-K_p$ from the lpg reference of 0.0016 to the 0.0025 case used by Kock and Herwig (not shown), there is an observable but small effect on the indirect or turbulent dissipation at low values of y^+.

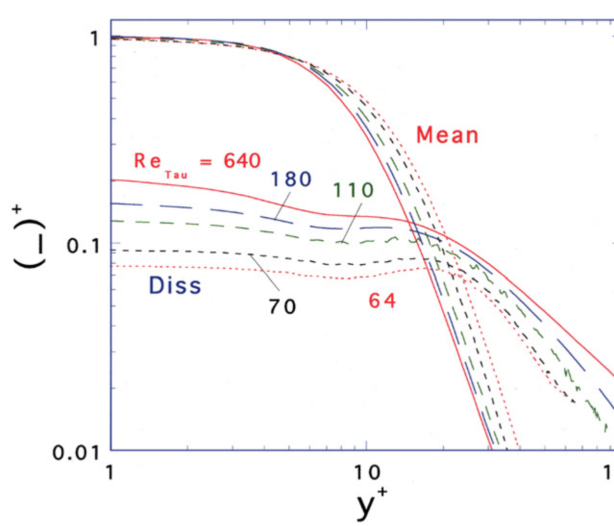

Fig. 4. Relative magnitudes of contributions to entropy generation with favorable pressure gradients occurring in low-Reynolds-number channel flow; same symbols for both families of curves.

The trends of the dissipation with respect to y^+ are the same as the pressure gradient varies but differ in magnitude. At each value of y^+ the turbulent dissipation decreases as pressure gradient increases. The turbulent dissipation ε^+ decreases slightly across a region from the wall to $y^+ \approx 15$. Then it decreases more sharply with y^+. For the lpg cases, by $y^+ \approx 20$ the turbulent dissipation is greater than the direct dissipation due to the mean motion; for the higher pressure gradients the two are of the same order until nearer the edge of the viscous layer. Direct dissipation is reduced to less than one per cent of the wall value of total dissipation by $y^+ \approx 40$ but by then ε^+ is significantly greater than the direct dissipation so $(S''')^+$ begins to become approximately equal to ε^+. Beyond $y^+ \approx 100$ for the lpg cases the distance to the edge of the boundary layer may still be large in wall units, but $(S''')^+$ is small so the contribution to entropy generation per unit surface area $(S'')^+$ is likewise small. These observations are consistent with those for the external boundary layer by McEligot et al. [15] but differ in detail and magnitudes at the same non-dimensional pressure gradients.

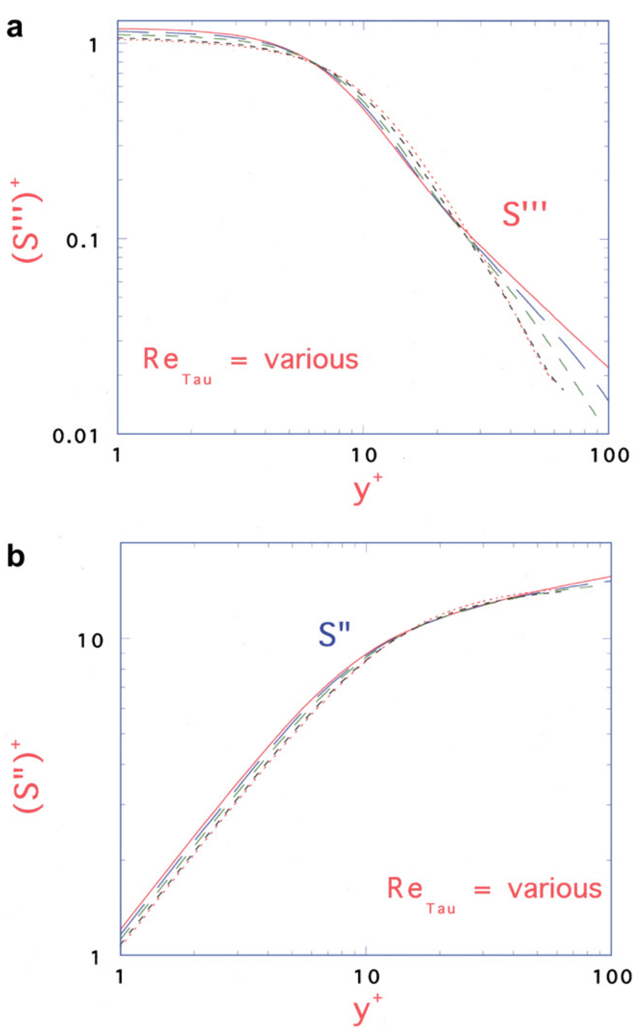

Fig. 5. Pointwise (a) and areal (b) entropy generation rates with favorable pressure gradients occurring in low-Reynolds-number channel flow; symbols as in Fig. 4.

The consequences of the countering effects on the two types of dissipation are plotted in terms of $(S''')^+$ and $(S'')^+$ in Fig. 5a and b and some key values are listed in Table 1. One sees, that the pressure gradient *does* affect entropy generation in the viscous layer but not to a large extent. In general, since the trends with respect to pressure gradient are in opposing directions for the mean and turbulent dissipations, the variations of $(S''')^+$ are less than of its individual components. And these variations lead to convergence of the curves for $(S'''\{y^+\})^+$ so they become nearly equal (crossing) near the edge of the viscous layer. As functions of y^+ the trends and orders-of-magnitude are the same as for the low pressure gradients of Figs. 2 and 3. Again S''' drops to less than 10% of its wall value by $y^+ = 30$ and over two-thirds or more of the entropy generation occurs in this viscous layer. From Table 1, one sees a variation of $(S''\{30\})^+$ from maximum to minimum of about 13% but, with the exception of the highest pressure gradient, the integration to $(S''\{30\})^+$ gives a range of only about 2%. This last observation has import for CFD analysts predicting entropy generation rates.

We *conclude* that non-dimensional entropy generation in the viscous layer ***is*** affected by a favorable pressure gradient but not to a great extent.

5. Application of viscous layer predictions

As suggested by Kock and Herwig [4,43], the direct numerical simulations for the viscous layer can be

Table 1
Effects of streamwise pressure gradients on entropy generation rates in turbulent channel flows

$-K_p$	0.00156	0.00253	0.00556	0.00667	0.00909	0.0125	0.0143	0.0156
$Re_\tau = y_c^+$	640	395	180	150	110	80	70	64
Re_{Dh}	48,900	28,300	11,400	9240	6580	4640	4040	3720
K_V	0	0	0	0	0	0	0	0
$U^+\{30\}$	13.55	13.67	14.02	14.05	14.64	15.32	15.81	16.25
$(S'''\{30\})^+$	0.0913	0.0906	0.0864	0.0859	0.0816	0.0808	0.0793	0.0833
$(S'''\{60\})^+$	0.0397	0.0388	0.0333	0.0316	0.0253	0.0208	0.0191	0.0187
$(S''\{30\})^+$	12.77	12.85	12.72	12.59	12.73	12.83	12.85	13.13
$(S''\{40\})^+$	13.54	13.61	13.43	13.30	13.39	13.45	13.44	13.75
$(S''\{50\})^+$	14.10	14.16	13.92	13.75	13.84	13.83	13.79	14.09
$(S''\{60\})^+$	14.54	14.59	14.30	14.15	14.15	14.08	14.02	14.31
$(S''\{y_c^+\})^+$	18.87	17.84	15.87	–	–	14.35	14.12	14.38

employed in conjunction with CFD codes which use wall functions and solve a partial differential equation for turbulent dissipation (ε_u here). Fig. 6a and b presents the behavior of the entropy generation rates S''' and S'' evaluated at $y^+ = 30$, the nominal edge of the viscous layer. (There appears to be slight numerical scatter, likely from the interpolations involved.) One sees that for both results there are slight differences between channel predictions and boundary layer predictions as the streamwise pressure gradients become large. Large pressure gradients correspond to low non-dimensional distances y_c^+ and δ^+, to the centerplane and the edge of the boundary layer, respectively. For these cases, it has been suggested that the outer turbulent flow region is not large enough for the viscous layer region to become insensitive to the outer boundary condition. Small K_p corresponds to high Reynolds numbers and viscous layers thin relative to the thickness of the turbulent region (i.e., distance to outer boundary). Thus, the channel and boundary layer results converge as $|-K_p|$ decreases.

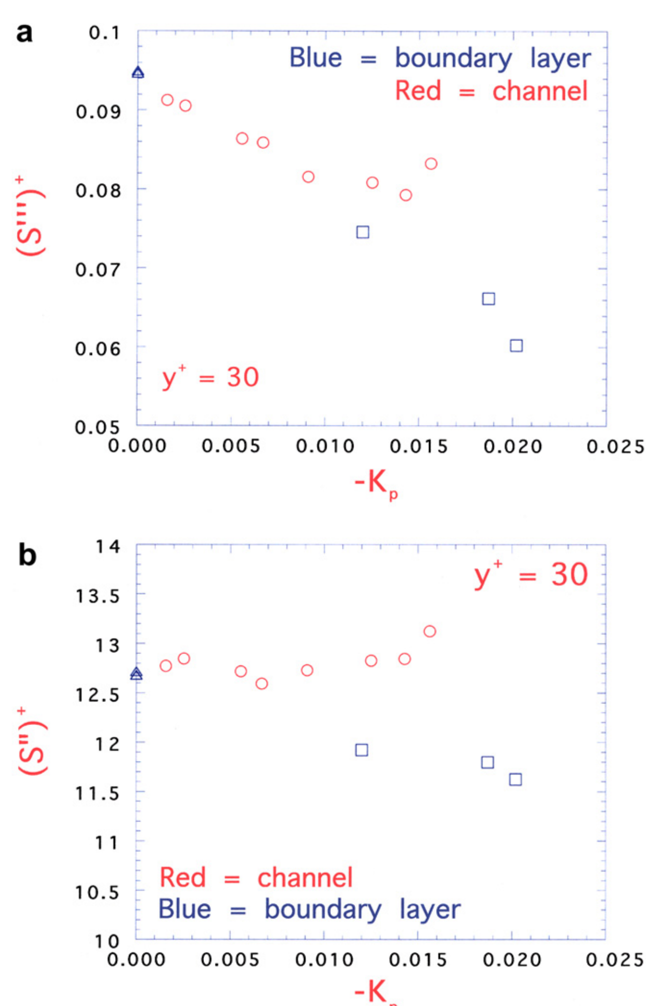

Fig. 6. Effects of streamwise pressure gradients on volumetric entropy generation rates at the edge of the nominal viscous layer (a) and entropy generation within the viscous layer per unit surface area (b) in fully-developed channel flow (circles) and in boundary layers on a flat plate (squares and triangles).

As fair approximations, one can represent the predictions at the nominal edge of the viscous layer ($y^+ = 30$) for favorable pressure gradients as

Pointwise entropy generation rate for channels with $-K_p < \sim 0.009$ and boundary layers with $-K_p < \sim 0.020$

$$(S'''\{30\})^+ \approx 0.095 + 1.7K_p$$

Areal entropy generation rate for channels with $-K_p < \sim 0.014$

$$(S''\{30\})^+ \approx 12.7 \quad (\pm 1\%)$$

and for boundary layers with $-K_p < \sim 0.020$

$$(S''\{30\})^+ \approx 12.65 + 50K_p$$

For fully-developed channel flows these limits correspond approximately to $Re_{Dh} > \sim 6600$ for S''' and $Re_{Dh} > \sim 4200$ for S'' or $y_c^+ > 110$ and 70, respectively. These approximate correlations for S'' are within 2% of each other for $-K_p < 0.004$ ($Re_\tau > 250$): this limitation is slightly less restrictive than the order-of-magnitude estimates suggested by McEligot and Eckelmann. With fully-developed flow in a duct of another cross section the asymptote would be the same but the variation with pressure gradient may vary slightly.

One of the main values of the comparisons in Fig. 6 is the indication when predictions of entropy generation from DNS of turbulent channel flows can and cannot be applied for the viscous layers of external turbulent boundary layers. The results for S'' in Fig. 6b demonstrate that the correlation suggested by Kock and Herwig [4] can be expected to predict the entropy generation within the viscous layer $(S''\{30\})^+$ reasonably for high Reynolds numbers and low pressure gradients although their value of $-K_p \approx 0.0025$ ($Re_\tau = 395$) is not quite an asymptotic situation. (Their non-dimensional quantity is comparable to our $(S'')^+$ but is defined differently.)

Ultimately, the thermal designer desires to predict S'', the entropy generation rate per unit surface area, for the turbulent flow of interest. A CFD code can provide $\partial U\{y\}/\partial y$ and $\varepsilon_u\{y\}$ beyond the node where the wall function is anchored; from these quantities $S'''\{y\}$ can be predicted beyond this node. The desired value is then given by

$$(S''\{y^+\})^+ = (S''\{y_1^+\})^+ + \int_{y_1^+}^{y^+} (S'''\{y^+\})^+ \mathrm{d}y^+$$

The value of S'' needed for an initial node at $y_1^+ = 30$ is given by Fig. 6b or the correlations. If the code anchors its wall function at a node closer than $y^+ = 30$, the required values of $\partial U/\partial y$ and ε_u can be estimated at $y^+ = 30$ by suitable interpolation (spline, logarithmic, quadratic or such) and then the integration can proceed to larger y^+. For $30 < y_1^+ < 60$, values can be interpolated from Table 1.

6. Concluding remarks

By employing results of direct numerical simulations it has been possible to examine entropy generation due to friction in the viscous layers of turbulent flows with significant streamwise pressure gradients, both for boundary layers and channels.

Entropy generation due to friction occurs from viscous dissipation of mean-flow kinetic energy (called "direct dissipation") and dissipation of turbulent kinetic energy into thermal energy ("indirect" or turbulent dissipation). We concentrate on the viscous layer because it is typically the region where the largest gradients occur and the production of turbulence is greatest; major resistances to momentum, energy and mass transfer occur in this layer – and the pointwise entropy generation rate is greatest here as well. (Here the viscous layer is defined as the region where viscous effects are significant, but not necessarily dominant; it includes the "laminar" and "buffer" sublayers in some investigators's terminology).

In wall coordinates the contribution of direct (mean) dissipation is unity at the wall. It dominates near the wall while turbulent dissipation contributes about 10–20% to the total. Both direct and turbulent dissipation decrease as y^+ increases but the reduction of direct dissipation is more rapid with respect to y than the turbulent dissipation – so they become about equal within the viscous layer. For larger values of y^+, turbulent dissipation becomes progressively more dominant. By the edge of the viscous layer the contribution of the mean motion is negligible.

For the viscous layer, DNS calculations for $Re_\theta \approx 1410$ without a pressure gradient are close to asymptotically-high Reynolds number conditions. The thickness δ^+ is about 650 so the viscous layer is small relative to the overall scale of the boundary layer and, therefore, is not expected to be affected significantly by the outer boundary condition. The non-dimensional total shear stress $\tau^+\{y^+\}$ is only reduced about 1–1/2% by the nominal edge of the viscous layer at $y^+ \approx 30$. This situation is close to the constant shear layer idealization which is valid for high-Reynolds-number flows. Thus, its distributions of $(S'''\{y^+\})^+$ and $(S''\{y^+\})^+$ would be approximately valid universally for the viscous layers of smooth wall flows at higher Reynolds numbers.

For a fully-developed channel flow, as the Reynolds number is increased the (non-dimensional) streamwise pressure gradient decreases and behavior in the viscous layer approaches that of the constant shear layer approximation. Consequently, such viscous layer results approach those of an asymptotic high-Reynolds-number boundary layer. Comparison of the DNS predictions for channel flow at $Re_\tau = 640$ ($-K_p \approx 0.0016$) with the DNS predictions for a zpg turbulent boundary layer at $Re_\theta \approx 1410$ confirms this expectation for the entropy generation distributions. The predictions of $(S'''\{y^+\})^+$ are very close to each other but differ slightly in detail. At these low pressure gradients about 30% of the entropy generation per unit surface area S'' occurs in the linear layer ($y^+ < \sim 5$) and about two-thirds or more occurs within the viscous layer.

With significant pressure gradients the viscous layer of a turbulent boundary layer is affected by the advection, by the outer boundary (since δ^+ is "small") and by the pressure gradient; with fully-developed channels, behavior in the viscous layer is affected by the pressure gradient and the other wall but not by advection. One sees that the pressure gradient *does* affect entropy generation in the viscous layer but not to a large extent. Increasing the pressure gradient increases the direct dissipation and decreases the turbulent dissipation. Consequently, the variations of $(S''')^+$ due to pressure gradients are less than of its individual components. As functions of y^+, the trends and order-of-magnitude are the same as for the low pressure gradients.

From examination of the results for channels and boundary layers with and without significant pressure gradients, one sees that – at the edge of the viscous layer – the pointwise entropy generation rate $(S'''\{30\})^+$ decreases as the favorable pressure gradient increases. However, the integral to this point $(S''\{30\})^+$ is relatively insensitive to pressure gradients for channels but decreases moderately for boundary layers. Approximate correlations are developed for potential use with CFD codes. At a pressure gradient of $-K_p \approx 0.004$, $(S''\{30\})^+$ for the boundary layer differs from the value for a channel by about 2%. Therefore, below this level, results based on DNS for a channel should be useful for external boundary layers provided $\delta^+ > \sim 600$. Above this level of pressure gradient separate predictions would be desirable for channels and boundary layers.

Acknowledgments

We are particularly grateful to Prof. Hiroshi Kawamura of Tokyo University of Science for his insight, guidance and use of his benchmark database on his Internet web site (http://murasun.me.noda.tus.ac.jp/). Dr. Suad Jakirlic of the Technische Universität Darmstadt kindly provided tabulations of the DNS results from Spalart [13,14]. The study reported was partly supported through Science Foundation Ireland. We thank the Director of IKE at Uni. Stuttgart, Prof. Dr. G. Lohnert, for his kind encouragement and support.

References

[1] A. Bejan, Entropy Generation through Heat and Fluid Flow, Wiley, New York, 1982.
[2] L. Onsager, Reciprocal relations in irreversible processes I, Phys. Rev. 37 (1931) 405–426.
[3] I. Prigogine, Time, structure and fluctuations, Science 201 (1978) 777–785.
[4] F. Kock, H. Herwig, Local entropy production in turbulent shear flows: a high-Reynolds number model with wall functions, Int. J. Heat Mass Transfer 47 (2004) 2205–2215.
[5] J. Kestin, Availability: the concept and associated terminology, Energy Int. J. 5 (1980) 679–692.
[6] M. Guoy, Sur l'energie utilisable, J. Phys. 8 (1889) 501–518.

[7] A. Stodola, Steam and Gas Turbines, McGraw-Hill, New York, 1910.
[8] S.O. Neumann, J. von Wolfersdorf, B. Weigand, A numerical study of entropy production rates in a film cooling configuration, GAMM (Gesellschaft für Angewandte Mathematik und Mechanik e.V.) (2005).
[9] R. Clausius, Die mechanische Wärmetheorie, Vieweg, Braunschweig, 1887.
[10] L.C. Lichty, Thermodynamics, McGraw-Hill, New York, 1936.
[11] P. Bradshaw, An Introduction to Turbulence and its Measurement, second ed., Pergamon, Oxford, 1975.
[12] H. Kawamura, H. Abe, Y. Matsuo, DNS of turbulent heat transfer in channel flow with respect to Reynolds and Prandtl number effects, Int. J. Heat Fluid Flow 20 (1999) 196–207.
[13] P.R. Spalart, Numerical study of sink-flow boundary layers, J. Fluid Mech. 172 (1986) 307–328.
[14] P.R. Spalart, Direct simulation of a turbulent boundary layer up to $Re_\theta = 1410$, J. Fluid Mech. 187 (1988) 61–98.
[15] D.M. McEligot, E.J. Walsh, E. Laurien, P.R. Spalart, Entropy generation in the viscous layers of turbulent boundary layers, in preparation.
[16] H. Abe, H. Kawamura, Y. Matsuo, Direct numerical simulation of a fully developed turbulent channel flow with respect to the Reynolds number dependence, J. Fluids Eng. 123 (2001) 382–393.
[17] T. Tsukahara, Y. Seki, H. Kawamura, D. Tochio, DNS of turbulent channel flow at very low Reynolds numbers, in: Proc., 4th Int. Symp. Turb. Shear Flow Phenomena, Williamsburg, VA, 27–29 June 2005, pp. 935–940.
[18] A.L. London, Advanced thermodynamics, Course ME 233, Stanford Univ., Fall, 1960.
[19] W.C. Reynolds, H.C. Perkins, Engineering Thermodynamics, McGraw-Hill, New York, 1970.
[20] T. Cebeci, P. Bradshaw, Physical and Computational Aspects of Convective Heat Transfer, Springer, New York, 1984.
[21] K. Gersten, H. Herwig, Strömungsmechanik, Vieweg, Braunschweig, 1992.
[22] H. Schlichting, K. Gersten, Grenzschicht-Theorie, 9., völlig neubearbeitete underweiterte Auflage, Springer, Berlin, 1997.
[23] H. Schlichting, K. Gersten, Boundary Layer Theory, eighth revised ed., Springer, Berlin, 2000.
[24] H. Schlichting, Boundary Layer Theory, sixth ed., McGraw-Hill, New York, 1968.
[25] R. Narasimha, K.R. Sreenivasan, Relaminarization of fluid flows, Adv. Appl. Mech. 19 (1979) 221–309.
[26] D.M. McEligot, H. Eckelmann, Laterally converging duct flows. Part 3. Mean turbulence structure in the viscous layer, J. Fluid Mech. 549 (2006) 25–59.
[27] S.J. Kline, W.C. Reynolds, F.A. Schraub, P.W. Rundstadler, The structure of turbulent boundary layers, J. Fluid Mech. 30 (1967) 741–773.
[28] V.C. Patel, Calibration of the Preston tube and limitations on its use in pressure gradients, Fluid Mech. 23 (1965) 185–208.
[29] J. Kim, P. Moin, R.D. Moser, Turbulent statistics in fully developed channel flow at low Reynolds number, J. Fluid Mech. 177 (1987) 133–166.
[30] H.L. Julien, W.M. Kays, R.J. Moffat, The turbulent boundary layer on a porous plate: experimental study of the effects of a favorable pressure gradient, Tech. Rpt. HMT-4, Thermosci. Div., Mech. Engr. Dept., Stanford Univ., 1969.
[31] D.S. Finnicum, T.J. Hanratty, Effect of favorable pressure gradients on turbulent boundary layers, A.I.Ch.E. Journal 34 (1988) 529–540.
[32] F.T.M. Nieuwstadt, P. Bradshaw, Similarities and differences in turbulent boundary-layer, pipe and channel flows, in: R.A.W.M. Henkes, P.G. Bakker (Eds.), Boundary-Layer Separation in Aircraft Aerodynamics, Univ. Press, Delft, 1997, pp. 15–22.
[33] V.E. Senecal, Fluid flow in the transition zone, Ph.D. thesis, Carnegie Inst. Tech., 1952.
[34] D.M. McEligot, L.W. Ormand, H.C. Perkins, Internal low Reynolds number turbulent and transitional gas flow with heat transfer, J. Heat Transfer 88 (1966) 239–245.
[35] B. Thiele, H. Eckelmann, Application of a partly submerged two component laser-Doppler anemometer in a turbulent flow, Exp. Fluids. 17 (1994) 390–396.
[36] F. Durst, M. Fischer, J. Jovanovic, H. Kikura, Methods to set up and investigate low Reynolds number, fully developed turbulent plane channel flows, J. Fluids Eng. 120 (1998) 496–503.
[37] J.O. Hinze, Turbulence, second ed., McGraw-Hill, New York, 1975.
[38] D.C. Wilcox, Turbulence Modeling for CFD, second ed., DCW Industries, La Canada, Cal, 1998.
[39] P. Bradshaw, J.B. Perot, A note on turbulent energy dissipation in the viscous wall region, Phys. Fluids A 5 (12) (1993) 3305–3306.
[40] R.A. Antonia, J. Kim, L.W.B. Browne, Some characteristics of small-scale turbulence in a turbulent duct flow, J. Fluid Mech. 233 (1991) 369–388.
[41] I. Wygnanski, M. Sokolov, D. Friedman, On transition in a pipe. Part 2. The equilibrium puff, J. Fluid Mech. 69 (1975) 283–304.
[42] R.B. Dean, Reynolds number dependence of skin friction and other bulk flow variables in two-dimensional rectangular duct flow, J. Fluids Eng. 100 (1978) 215–222.
[43] F. Kock, H. Herwig, Entropy production calculation for turbulent shear flows and their implementation in cfd codes, Int. J. Heal Fluid Flow 26 (2005) 672–680.